Journal of Power Sources 240 (2013) 796–805

Contents lists available at SciVerse ScienceDirect

Journal of Power Sources

journal homepage: www.elsevier.com/locate/jpowsour

# Effect of contact area and depth between cell cathode and interconnect on stack performance for planar solid oxide fuel cells☆

Le Jin, Wanbing Guan**, Jinqi Niu, Xiao Ma, Wei Guo Wang*

*Ningbo Institute of Material Technology & Engineering, Chinese Academy of Sciences, 519 Zhuangshi Road, Ningbo 315201, China*

## HIGHLIGHTS

- Convex parabolic relation of power density vs. interface contact area and depth was found.
- The degradation rate of stack repeat unit decreased gradually with the increasing contact area.
- The stack repeat unit inside stack appears no degradation with the increasing contact depth.

## ARTICLE INFO

*Article history:*
Received 5 February 2013
Received in revised form
3 April 2013
Accepted 8 April 2013
Available online 18 April 2013

*Keywords:*
Contact area
Contact depth
Degradation rate
Stack
Solid oxide fuel cell

## ABSTRACT

Effect of contact area and depth between cell cathode and interconnect on output power density and degradation of stack for planar SOFCs has been investigated systematically. The results indicate that the maximum output power density (MOPD) of repeating units inside stack increases firstly and then decreases slightly with the increasing interface contact area and depth, respectively, showing an approximate convex parabolic relation of power density to interface contact area and depth. The degradation rate of repeating units decreases gradually for 972 h' operation under 0.75 V unit-cell voltage, 0.476 A cm$^{-2}$ current density and 41.8% fuel utilization with different contact area. At the optimum value of the interface contact area, the repeating unit inside stack appears no degradation under operation for 1060 h under 0.8 V unit-cell voltage, 0.444 A cm$^{-2}$ current density, and 78% fuel utilization efficiency.



## 1. Introduction

Solid oxide fuel cells (SOFCs) are highly efficient energy conversion devices. To obtain applicable electric energy, unit cells must be connected in series to form a cell stack [1]. The SOFC stack structure shows that the performance is mainly influenced by metal interconnects, unit cells, and interfaces between unit cells and metal interconnects. For many years, the cell performance has been considered as the fundamental influencing factor for SOFC stack; thus, improving the cell performance has always remained a research interest [2–4]. However, when a high-performance unit cell is used, the SOFC stack still has significantly poorer performance than the unit cell itself [5]. This result indicates the importance of investigating the performance of the interconnect for SOFC stack. According to research findings, if metal materials are used as interconnects for SOFC stack, the resistance of the interconnect is still small under 700 °C–850 °C, and its influence on the output performance of the whole cell stack is almost negligible [6–8]. The interface contact between metal interconnect and unit cell is currently recognized as the key factor influencing the performance of SOFC stack [9,10].

The interface contact between SOFC stack components mainly comes from two aspects: (1) the interface contact between anode and interconnect, and (2) the interface contact between cathode and interconnect. For SOFC stack, the anode functions as a metal material under an operating condition. Therefore, metal–metal contact is mainly on the anode side of the stack. The contact resistance on anode side is almost negligible after full contact is made [11]. Research has also discovered that the contact resistance in SOFC stack mainly comes from the interface contact between cell cathode (perovskite material) and metal interconnect [12–14].



* Corresponding author. Tel.: +86 574 8791 1363.
** Corresponding author. Tel.: +86 574 8668 5137.
*E-mail addresses:* wbguan@nimte.ac.cn (W. Guan), wgwang@nimte.ac.cn (W.G. Wang).

0378-7753/$ – see front matter © 2013 The Authors. Published by Elsevier B.V. All rights reserved.
http://dx.doi.org/10.1016/j.jpowsour.2013.04.027

Thus, to minimize the resistance produced by the interface contact between cell cathode and interconnect, precious metals such as Pt and Ag are used as the current collecting materials on the cathode side [11,15]. Using precious metals as the cathode current collector can provide the cell with higher output power density. However, their high material costs highly limit their large-scale commercial application in SOFC.

The interface contact area between the cell cathode and interconnect is a key factor influencing the output performance for SOFC stack [16–18]. Therefore, with the same materials selected as the cathode current collecting layer (CCCL), increasing the interface contact area between the cell cathode and metal interconnect can significantly increase the power density of the cell inside SOFC stack. For example, the research findings of Jiang et al. [16] in 2003 showed that when the contact area of the cell cathode grew from 5% to 27.5%, the maximum output power density (MOPD) of the cell correspondingly increased from 0.10 W $cm^{-2}$ to 0.52 W $cm^{-2}$. However, according to the report, the contact area varied within the range of 5%–27%, and the cell area was relative small (5 cm × 5 cm), which were some of the limitations. Furthermore, no research exists on the relationship between the interface contact area and the degradation rate of the cell in the literature [16]. Our preliminary study [19] also provided that the MOPD of the cell inside SOFC stack is related to the interface contact area and contact depth between cell cathode and interconnect. Based on the aforementioned findings, the degradation rate of the cell inside stack shows a direct relationship with the interface contact [20]. However, quantitative research on the relationship of the contact depth between the cell cathode and the metal interconnect with the output performance, especially the relationship with the degradation rate, is severely limited.

This study is a quantitative research on the relationship between interface contact area and depth, as well as between MOPD and degradation rate, by varying the contact area and depth between the cell cathode and the metal interconnect. A preliminary discussion on the specific mechanism is included, providing useful reference for the research and development of an SOFC stack with high power density and low degradation rate.

## 2. Experimental methods

The anode-supported NiO–YSZ/YSZ/LSM–YSZ unit cells were used in this experiment. The manufacturing process and parameters of the cell are described in detail in the literature [21,22]. In this experiment, the cell size in our stack was 10 cm × 10 cm with an active cathode area of 63 $cm^2$. Cells were machined to the required size by laser cutting. To realize the full contact between cell anode and metal interconnect, a NiO layer of about 130 μm was printed on the anode side of the cell by screen printing. After drying, a layer of about 250 μm $(La_{0.75}Sr_{0.25})_{0.95}MnO_3$ (LSM) was printed on the cell cathode side by the same method. A stack was assembled according to the schematic diagram, as shown in Fig. 1, in which the metal interconnect was 430 ferritic stainless steel and the sealing material was $Al_2O_3$–$SiO_2$–CaO based glass. The performance of the sealing materials is described in the literature [23].

On the anode side of the metal interconnect, a kind of linear-type gas channel was prepared by etching with a depth of about 0.5 mm. On the cathode side of the metal interconnect, metal mesh was used as gas channel and electron collector. The structure of the metal mesh was designed and prepared by punching according to the reported references [24–26], as shown in Fig. 2. In this work, Ni-based alloy material was applied and manufactured as metal mesh, which was welded on the metal interconnect. To prevent high-temperature oxidation and Cr element volatilization, a layer of Ni–Cr/LSM composite coating was sprayed on the cathode side of the metal interconnect by plasma spraying technique. The relevant process indexes can be found in the literature [20].

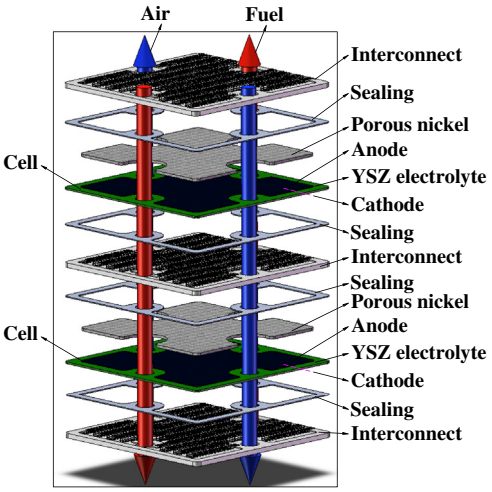


**Fig. 1.** Schematic diagram of stack assembling.

To study the influence of interface contact area on the output power density and degradation performance of the repeating unit (containing a piece of interconnect and a piece of unit cell) and unit cell inside stack, the interface contact area between the metal interconnect and the cell cathode was designed through adjusting the width and amount of protrusions on metal mesh, as seen in Fig. 2. The interface contact between the metal interconnect and the cell cathode mainly occurred through the protrusion on the metal mesh. Therefore, when the metal mesh made full contact with the cell cathode, the interface contact area was equal to that of the protrusion on the metal mesh. Thus, the interface contact area can be changed by varying the width and number of protrusions on the metal mesh, i.e., varying the values of $a$ (width of metal mesh), $N_1$ and $N_2$ (amount of protrusions on meal mesh) in Fig. 2). With this interface contact method, the theoretical contact areas were designed as 28.17%, 33.39%, 38.84% and 45.37%, respectively, according to the stack structure shown in Fig. 1. The corresponding parameters were listed in Table 1.

Based on these contact areas, a first 4-cell stack (called stack 1) was assembled to conduct the test. In the stack assembly process, the voltage leads were led out from the anode side and cathode side of the cell, respectively, as shown in Fig. 3. With the voltage leads on both sides of the cell, the independent voltage curve could be obtained for each component inside the stack in the operating

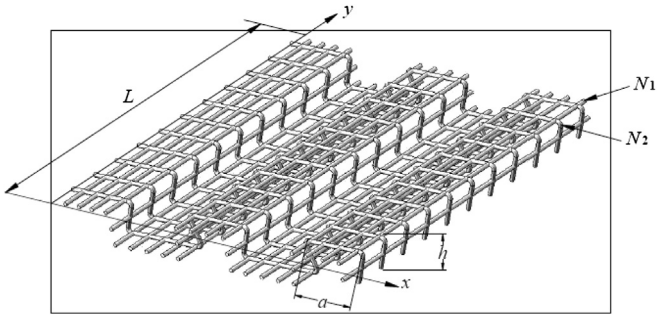


**Fig. 2.** Schematic diagram of metal mesh on cathode side: $a$–the contact width of metal mesh; $L$–the total length of metal mesh; $h$–the height of metal mesh; $N_1$–the amount of metal mesh in $y$ direction; $N_2$–the amount of metal mesh in $x$ direction.

**Table 1**
The parameters of metal mesh on cathode side.

| Cell no. | $a$/cm | $L$/cm | $N_1$ | $N_2$ | $d$/cm | $S_{contact}$/cm$^2$ | $S_{active}$/cm$^2$ | $S$/% |
|---|---|---|---|---|---|---|---|---|
| 1 | 0.4 | Constant | 32 | 43 | Constant | 17.85 | 63 | 28.17 |
| 2 | | | 32 | 60 | | 21.25 | | 33.39 |
| 3 | 0.5 | | 46 | 43 | | 24.06 | | 38.84 |
| 4 | | | 46 | 60 | | 28.56 | | 45.37 |

process, which facilitated the performance analysis on each component inside the stack.

As shown in Fig. 2, the interface contact between the metal interconnect and cell cathode was partially realized through the protrusion on the metal mesh. Therefore, the contact depth design could be realized by changing the height of protrusions on the metal mesh, i.e., changing $h$ in Fig. 2. By punching, the height $h$ of the protrusion on the metal mesh could reach 250, 150, 100, and 30 μm, respectively. A second 4-cell stack (named stack 2) was assembled to conduct the test. In stack 2, the contact area between the cell cathode and the metal interconnect was equal to the optimum value of the contact area, as indicated by the test of stack 1. In the testing procedure, the voltage leads were led out from both sides of the cell according to the schematic diagram shown in Fig. 3.

After the assembly, the stack was placed on a heating furnace and was heated to 850 °C at the rate of 1 °C min$^{-1}$. The temperature remained unchanged for about 2 h. For stack sealing, an external pressure of about 10 N cm$^{-2}$ was loaded on the stack in heat preservation. Fig. 4 shows the schematic diagram for applying pressure in stack testing. The stack was then cooled to the working temperature of 800 °C before testing. In the testing process, the anode side of the stack was subjected to nitrogen purging for 5 min–10 min, and then hydrogen and air were fed into the anode and the cathode of the stack, respectively. The test began after the cell anode underwent more than 3 h of reduction in a hydrogen atmosphere. The testing results are presented below. After electrical testing, morphology and microstructure were investigated to verify the contact design by SEM (Hitachi S-4800).

## 3. Results and discussion

### 3.1. Effect of contact area on power density and degradation

In order to calculate the contact area between interconnect and cell cathode inside stack 1, the surface morphology of contact traces left on CCCL by the mesh protrusions of the metal interconnect after testing was characterized, as shown in Fig. 5. It can be seen clearly the CCCL of the stack and the mesh protrusions of the metal interconnect were almost in a state of full contact. The results show that the actual contact area almost exactly matched the contact

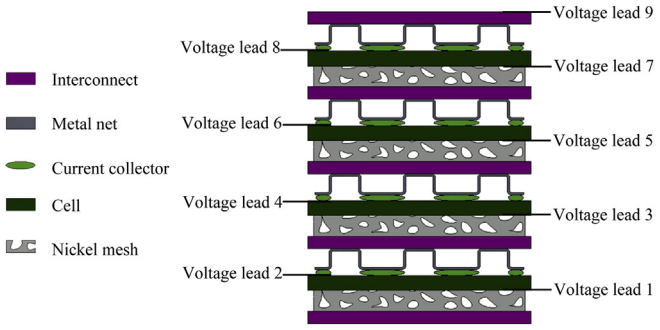


**Fig. 3.** Schematic diagram of voltage leads arranged inside stack.

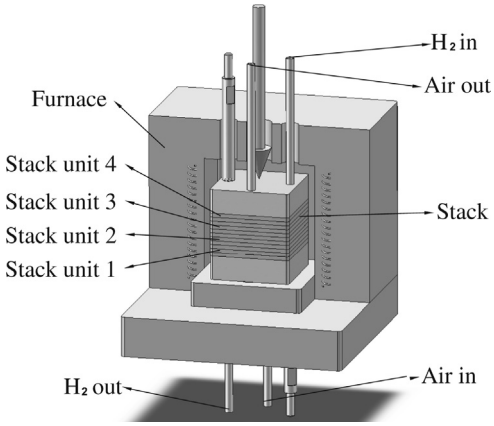


**Fig. 4.** Schematic diagram of load and gas flow during stack testing.

area in the theoretical design. Thus, the contact areas corresponding to the cathode side of cells 1, 2, 3, and 4 in the stack were 28.17%, 33.39%, 38.84% and 45.37%, respectively.

Fig. 6a) shows the $I$–$V$ curve of stack 1 under 800 °C. The result shows that the open circuit voltage (OCV) for this 4-cell stack was 4.614 V and the MOPD was 0.428 W cm$^{-2}$, which indicates that the MOPD was 108.465 W. The stack had a high sealing and output power density performance. Fig. 6b) shows the testing results of the $I$–$V$ curve for the repeating unit (interconnect + unit cell) and that for the corresponding unit cell in the stack. The results in the graph show that the OCVs of the repeating unit 1, 2, 3, and 4 were 1.147, 1.168, 1.170, and 1.152 V, respectively, and the corresponding MOPDs were 0.315, 0.428, 0.496, and 0.482 W cm$^{-2}$, respectively. The OCVs for the unit cell in the stack were 1.146, 1.168, 1.162, and 1.153 V, respectively, and the corresponding MOPDs were 0.392, 0.459, 0.515, and 0.506 W cm$^{-2}$, respectively. In the stack, the OCVs of the repeating unit and the unit cell were close to or higher than 1.15 V, suggesting a state of perfect sealing for each unit component in the stack. The OCVs of both sides of the repeating unit were equal to those of the unit cell, but the MOPD was slightly lower than that of the unit cell.

Fig. 7 shows the variation pattern of the MOPD of the unit cell in the stack changing with the interface contact area. The results in the graph show that when the interface contact area between the cell cathode and the metal interconnect increased from 28.17% to 38.84%, the MOPD of the unit cell in the stack also increased. When the contact area was 38.84%, which was higher than that of unit cell 1 (28.17%) by 9.86%, the MOPD increased by 56.3%. The results in the graph also show that when the contact area continued to increase from 38.84% to 45.37%, the MOPD showed a slight decrease, not an increasing tendency. The MOPD of repeating unit and unit cell seems to have an approximate convex parabolic relation vs. contact area between interconnect and cell cathode. Therefore, within a certain range of contact area at the cathode, the contact area has a significant effect on the MOPD of the repeating unit and the corresponding cell. The larger the contact area, the better the effect of electron collection, and the higher the MOPD. This result agrees with the result obtained by Jiang [16] and Guan [19] et al., though their results were obtained by conducting different stacks. However, in the report of Jiang et al. [16], the contact area between the cell cathode and the metal interconnect varied within the range of 5%–27%.

The difference between the $I$–$V$ curve results for the unit cell in the stack and the $I$–$V$ curve results for the repeating unit was obtained. Thus, the changing relationship with the current density magnitude was established (Fig. 8). This curve shows the

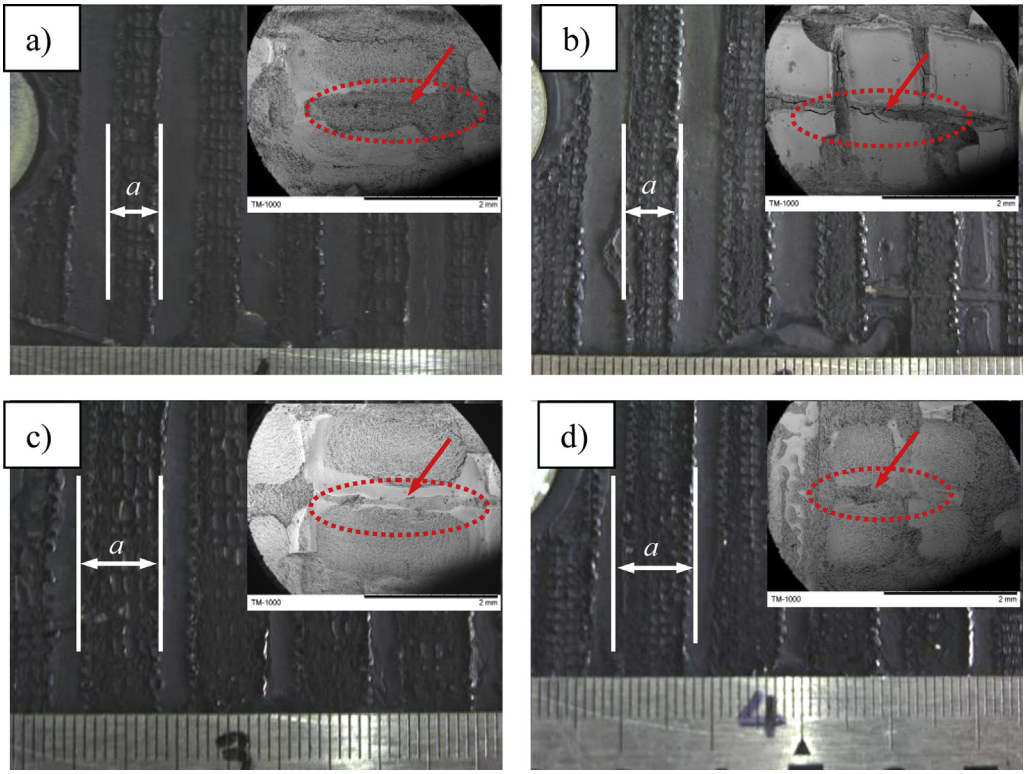


**Fig. 5.** Surface morphology of contact traces left on the cathode current collecting layer: (a) cell 1—28.17%, (b) cell 2—33.39%, (c) cell 3—38.84% and (d) cell 4—45.37%.

relationship of the change in the sum of voltage drop (named $\Delta U_{IC}$) produced by the metal interconnect and the interface contact with the current density magnitude. As the graph shows, these two parameters exhibited a linear relationship. After fitting, the slope was calculated as 0.0998, 0.0449, 0.0351, and 0.0297, respectively. The results show that the sum of the area specific resistance (ASR) of metal interconnect corresponding to repeating units 1, 2, 3, and 4 and the contact resistance with the cell cathode (named $ASR_{IC1}$, $ASR_{IC2}$, $ASR_{IC3}$ and $ASR_{IC4}$) was 99.8, 44.9, 35.1 and 29.7 mΩ $cm^{-2}$, respectively. When the interface contact area increased from 28% to 45%, $\Delta R_{IC}$ first decreased and then increased. Therefore, this result is the major cause of the increase-and-then-decrease trend of the MOPD of the repeating unit inside stack.

A degradation performance study was also conducted on this stack. A degradation performance test was conducted on this stack with a constant current density of 0.476 A $cm^{-2}$ (current 30 A) and a fuel utilization efficiency of 41.8% (Fig. 9a). Under this condition, the initial operating voltage of the stack was 2.83 V (repeating unit 0.7 V) and the operating power was 84.86 W. The stack underwent nearly 150 h of activation, after which the operating voltage increased to 3.061 V (0.765 V for the repeating unit) and the operating power increased to 91.9 W. After the activation stage, the stack entered the stage of stable operation that lasted for 822 h. During the 822 h of stable operation, the degradation rate for the stack was 3.1%/1000 h. Fig. 9b) shows the degradation curve for the operating repeating unit. The results show that the voltage degradation rates corresponding to repeating units 1, 2, 3, and 4 were 3.02%/1000 h, 3.25%/1000 h, 3.37%/1000 h and 2.28%/1000 h, respectively. This result indicates that with increasing interface contact area, the degradation rate first increased and then decreased, and when the interface contact area was 45%, the degradation rate reached its minimum value.

In the operating process of the stack, the changing OCV of the stack and the repeating unit were observed by temporarily suspending the discharge. The OCV for the stack was 4.617 V at the initial stage of constant-current operation, 4.676 V at 258 h, 4.694 V at 895 h, and 4.702 V at 972 h, as listed in Table 2. The OCV for the stack underwent a slight increase with the extension of the operation time. The OCVs for repeating units 1, 2, 3, and 4 at different operating stage were listed in Table 3. The results show that the stack and the repeating unit had a perfect sealing performance in the operation process and were not the factors leading to degradation.

Fig. 10 shows the voltage degradation curve of unit cell in the stack. The voltage degradation rates corresponding to unit cells 1, 3, and 4 in the stack were 6.16%/1000 h, 3.77%/1000 h, and 1.49%/1000 h, respectively. The voltage of cell 2 showed fluctuations in the operation process, so no degradation occurred. Thus, with increasing interface contact area, the degradation rate of the unit cell slowly decreased and reached the bottom at the contact area of 45%. The OCVs for unit cells 1, 2, 3, and 4 at different operating stage were listed in Table 4. As seen in Table 4, it can be found that the OCV for the unit cell in the stack almost remained constant, indicating that the sealing was not the cause of cell degradation.

Fig. 11 shows the voltage drop ($\Delta U_{IC}$) jointly contributed by the metal interconnect and its interface contact with the cell cathode. In the operation period, the voltage drop ($\Delta U_{IC}$) caused by the metal interconnect in the stack and its interface contact with the cell cathode was always constant, without showing any increasing trend. Fig. 11 also shows that under the current density of 0.476 A $cm^{-2}$ (30 A current), the greatest voltage drop ($\Delta U_{IC1}$) was caused by the metal interconnect in repeating unit 1 and its interface contact with cell cathode, followed by that in repeating units 2, 3, and 4 ($\Delta U_{IC2}$, $\Delta U_{IC3}$, and $\Delta U_{IC4}$).

Therefore, the stack degradation during the operation process is caused by the degradation in cell performance, whereas the cell performance degradation rate is inversely proportional to the contact area with the cell cathode. The larger the interface contact area, the smaller the performance degradation rate of the cell.

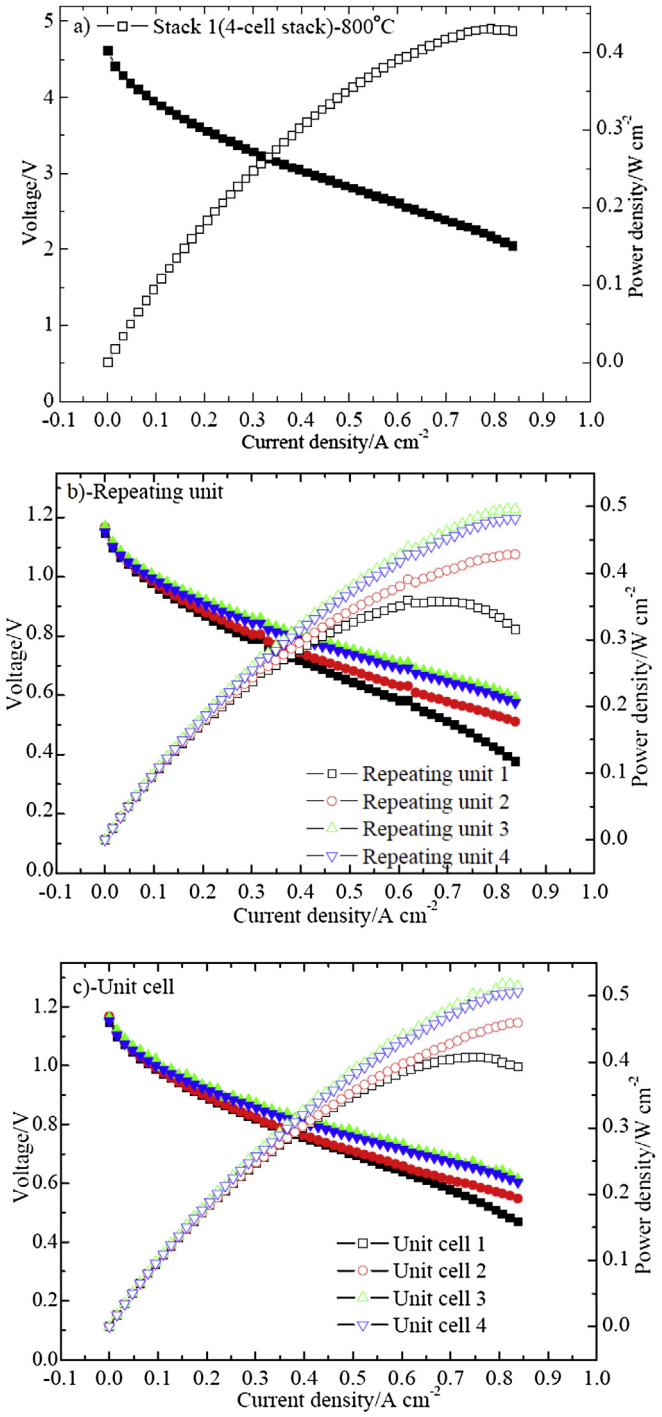


**Fig. 6.** *I–V* curves of stack 1 and its corresponding repeating unit and unit cell: (a) stack 1, (b) repeating unit, (c) unit cell.

Compared with the cell performance degradation, the degradation rate for the repeating unit in the stack increases as the interface contact area rises from 28% to 39%. When the interface contact area further grows to 45%, the degradation rate for the repeating unit begins to drop and reaches the minimum.

### 3.2. Effect of contact depth on power density and degradation

In order to investigate the contact depth on the performance of unit cell and repeating unit inside stack 2 during operation, the cross-section morphology for each cell in stack 2 after testing was observed, as seen in Fig. 12. The marked area represents the morphology of the traces left by the contact between the metal mesh and the CCCL. The graph shows the contact depth between the CCCL of each unit cell and the interconnect. The results in Fig. 12 show that the actual values for contact depth between the metal interconnect in the stack and the CCCL of cells 1, 2, 3, and 4 are 226, 120, 105, and 38 μm, respectively, which are slightly different from the values in the theoretical design.

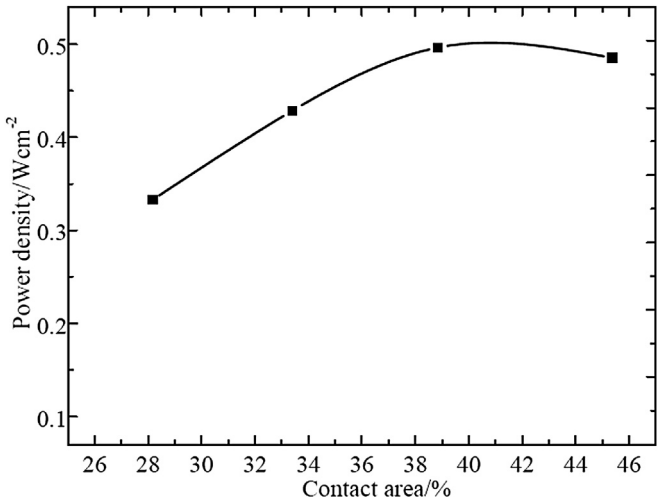


**Fig. 7.** The relationship between the cell MOPD in stack and the interface contact area.

Fig. 13 shows the *I–V* curves for stack 2 and its repeating unit and unit cell. The results of Fig. 13a) show that with a hydrogen flow of 7.9 sccm $cm^{-2}$, the OCV for the stack was 4.684 V and the MOPD was 0.519 W $cm^{-2}$. The results in Fig. 13b) show that the OCVs for repeating units 1, 2, 3, and 4 were 1.153, 1.166, 1.168, and 1.152 V, respectively, and the corresponding MOPDs were 0.456, 0.540, 0.548, and 0.538 W $cm^{-2}$, respectively. The results in Fig. 13c) show that with a contact depth of 226, 120, 105, and 38 μm, the corresponding OCVs for the unit cell were 1.153, 1.166, 1.167, and 1.152 V, respectively, whereas the MOPDs were 0.489, 0.544, 0.571, and 0.563 W $cm^{-2}$, respectively. Therefore, when the interface contact depth is 228 μm, the corresponding MOPD of repeating unit drops

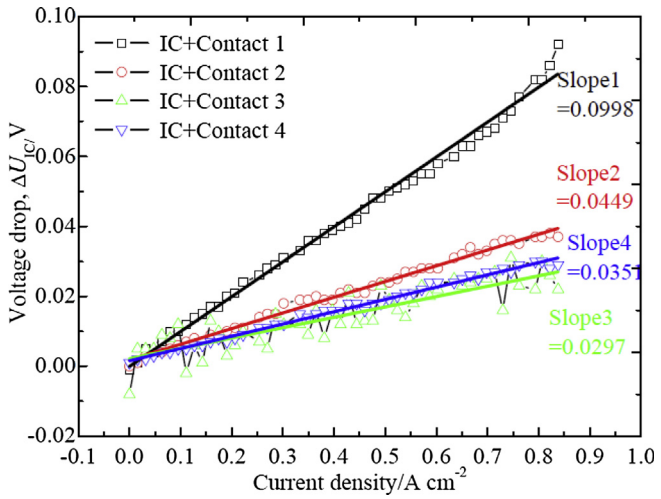


**Fig. 8.** The correlation of voltage drop caused by metal interconnect and interface contact to the current density magnitude.

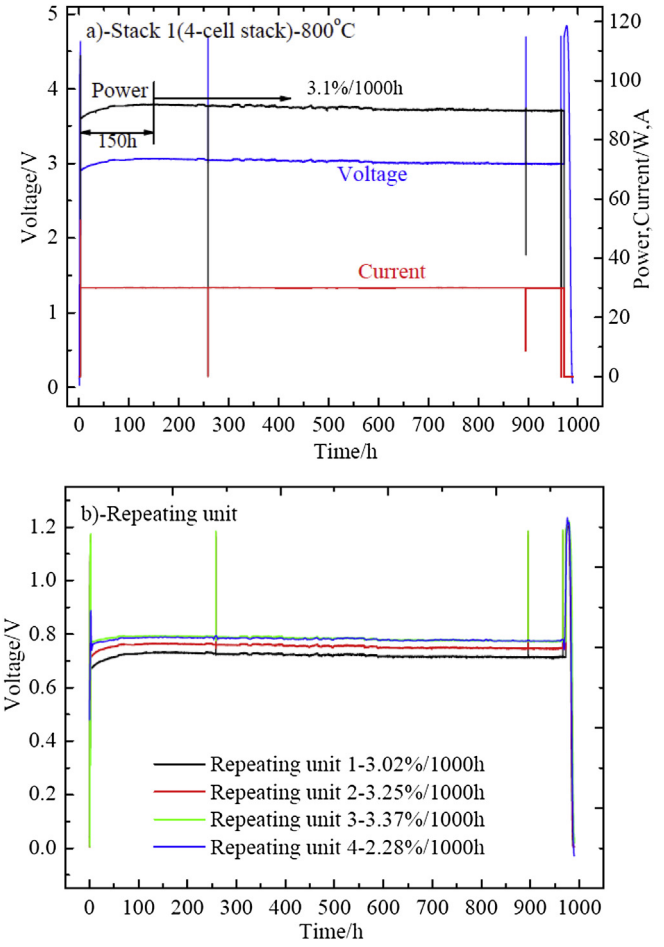


**Fig. 9.** Degradation curve of stack 1 and its corresponding repeating unit: (a) stack 1, (b) repeating unit.

to its minimum at 0.456 W $cm^{-2}$. As the interface contact depth decreases, the MOPD of the repeating unit slightly increases. As the same as the results obtained by designing contact area, an approximate convex parabolic relation of power density vs. contact depth between interconnect and cell cathode was also found. When the interface contact depth decreases to 105 μm, the MOPD of the repeating unit rises to its maximum at 0.548 W $cm^{-2}$. In our previous published research [19,20], it was found that the cell performance with deep contact is much better than that with shallow contact between interconnect and cell cathode inside stack by conducting electrochemistry testing of different stacks with the same contact area. The results in this work show that an optimum

**Table 2**
The OCV of stack 1 at different operation time, *V*.

| 0 h | 258 h | 895 h | 972 h |
|---|---|---|---|
| 4.617 V | 4.676 | 4.694 | 4.702 |

**Table 3**
The OCV of repeating unit inside stack 1 at different operation time, *V*.

| Time | 0 h | 258 h | 895 h | 972 h |
|---|---|---|---|---|
| 1 | 1.149 | 1.163 | 1.170 | 1.171 |
| 2 | 1.168 | 1.181 | 1.185 | 1.186 |
| 3 | 1.171 | 1.186 | 1.186 | 1.188 |
| 4 | 1.154 | 1.168 | 1.170 | 1.173 |

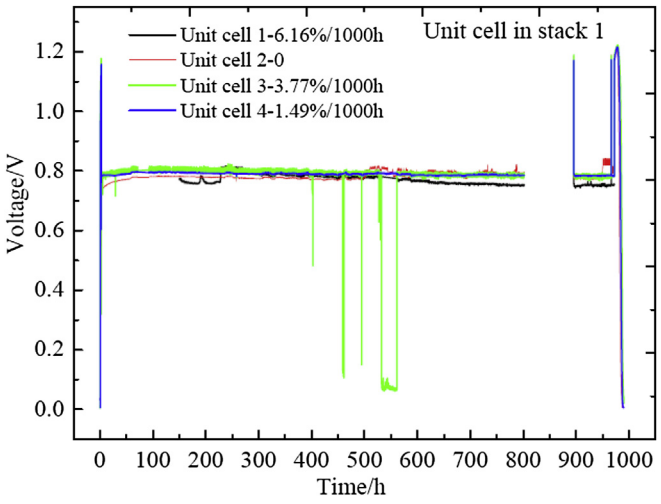


**Fig. 10.** Degradation curve of the unit cell in stack 1.

value for the contact depth between cell cathode and metal interconnect exists, which is approximately 105 μm under the condition of this experiment, as shown in Fig. 14.

The difference between the *I*–*V* curve of the unit cell in the stack and that of the repeating unit was obtained to establish the changing curve with current density magnitude (Fig. 15). This curve shows the change in the relationship of the voltage drop ($\Delta U_{IC}$) jointly caused by the metal interconnect and its interface contact with the cell cathode as current density magnitude varies, as these two factors are linearly proportional. After fitting, the slopes are calculated as 0.0421, 0.0286, 0.0195, and 0. 0051, respectively. The results show that the sum of the ASR ($ASR_{IC1}$, $ASR_{IC2}$, $ASR_{IC3}$, and $ASR_{IC4}$) produced by the metal interconnect corresponding to repeating units 1, 2, 3, and 4 and its interface contact with the CCCL is 42.1, 28.6, 19.5 and 5.1 mΩ $cm^{-2}$, respectively.

Therefore, when the interface contact depth is 228 μm, the sum of the ASR produced by the metal interconnect and its interface contact with the cell cathode reaches its maximum, corresponding to the smallest MOPD. When the interface contact depth continues to decrease, the sum of the ASR produced by the metal interconnect corresponding to repeating units 3 and 4 and its interface contact with the cell cathode decreases, but not repeating unit 2. However, the MOPD reaches its largest value under 105 μm. When the sum of the ASR produced by the metal interconnect and the interface contact decreases to a specific value, this sum has less influence on the MOPD of the cell. Comparing the results in Fig. 15 with that in Fig. 8, it can be find that the ASR of the metal interconnect and interface contact generally decreases regardless of the contact depth when the interface contact area is 45%. However, a substantial increase in the MOPD for the stack and its repeating unit and unit cell was observed (Figs. 7 and 14).

After *I*–*V* curve testing of stack 2, the constant-current discharge and charge test under a hydrogen flow of 4 sccm $cm^{-2}$ and a current density of 0.444 A $cm^{-2}$ (current 28 A) were conducted, as seen in

**Table 4**
The OCV of unit cell inside stack 1 at different operation time, *V*.

| Time | 0 h | 258 h | 895 h | 972 h |
|---|---|---|---|---|
| 1 | 1.147 | 1.162 | 1.168 | 1.169 |
| 2 | 1.169 | 1.181 | 1.187 | 1.186 |
| 3 | 1.178 | 1.184 | 1.190 | 1.187 |
| 4 | 1.155 | 1.168 | 1.171 | 1.174 |

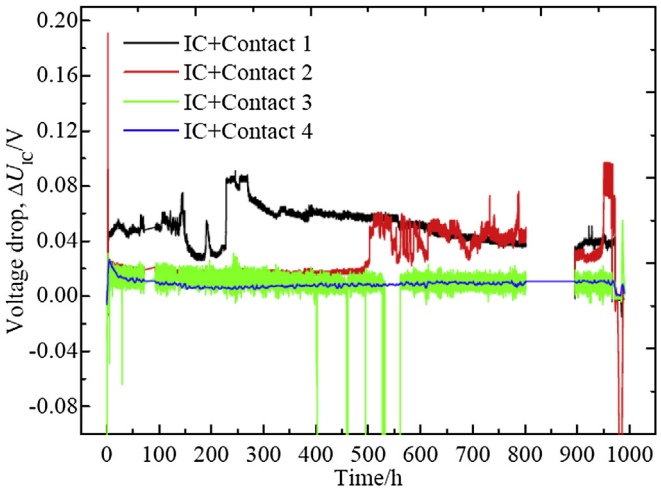


**Fig. 11.** Voltage drop contributed by the interconnect and its contact with the cell cathode.

Fig. 16. Under this condition, the fuel utilization efficiency for the stack is 78%. The initial operating voltage of the stack is 3.0 V (0.75 V for repeating unit or unit cell) and the operating power is 84 W. After undergoing an activation stage that lasted for nearly 150 h, the operating voltage is 3.22 V (the voltage for repeating unit or unit cell increased to 0.805 V) and the operating power is 90.17 W. At this time, the stack enters the stage of continuous stable operation. Fig. 16a) shows that during 910 h of operation, hardly any degradation can be detected. Thus, the degradation rate is 0. Fig. 16b) and c) show the operation curves for the repeating unit and its unit cell. The results also show that the repeating unit and its unit cell do not show any degradation.

Fig. 17 shows the changing curve of the voltage drop ($\Delta U_{IC}$) jointly contributed by the metal interconnect and its interface contact with the cell cathode in the operation process of the stack. The results also show that in the operation process of the constant-current discharge of the stack, the voltage drop ($\Delta U_{IC1}$, $\Delta U_{IC2}$, and $\Delta U_{IC4}$) jointly contributed by the metal interconnect corresponding to repeating units 1, 2, and 4 and its interface contact with cell cathode remains stable, showing without any increase. Moreover, almost all values are below 20 mV. When repeating unit 3 operates to 250 h, a sharp increase is observed, after which the value stabilizes at the point of $\leq$45 mV. The voltage drop ($\Delta U_{IC}$) jointly contributed by the metal interconnect in stack 2 and its interface contact with the cell cathode (Fig. 17) is similar to that in stack 1 (Fig. 11) in terms of variation trend and magnitude. Therefore, the stable performance of the metal interconnect and its interface contact with cell cathode is one of the key factors that can guarantee the absence of degradation in the stack. At the initial stage and the end stage of the operation of the stack, the OCVs for the cell stack are 4.629 and 4.745 V, respectively. At the initial stage of the operation, the OCVs for repeating units 1, 2, 3, and 4 are 1.148, 1.161, 1.163, and 1.143 V, respectively, whereas after the operation, the OCVs for the repeating units are 1.187, 1.188, 1.185, and 1.172 V, respectively. Similarly, the sealing of the stack improves with time. An important reason why no degradation occurs in the stack at the operation stage is due to its excellent sealing performance.

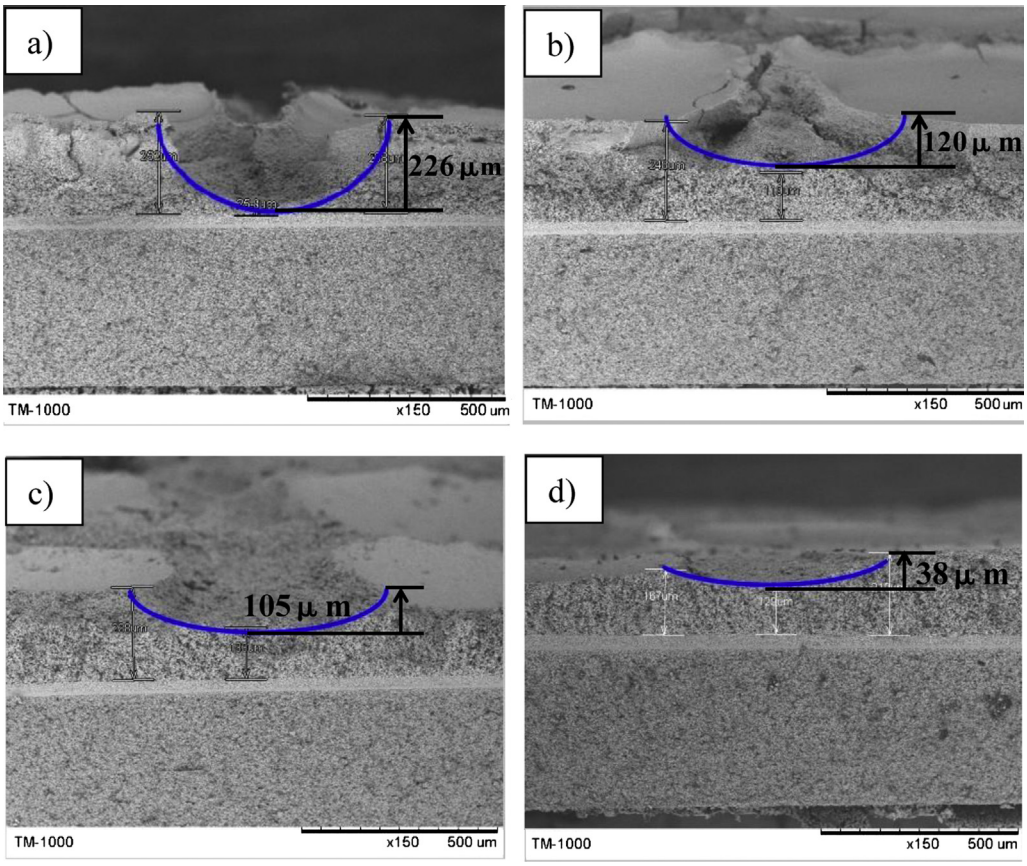


**Fig. 12.** The cross-section morphology of each cell in stack 2: (a) cell 1–226 μm in depth, (b) cell 2–120 μm in depth, (c) cell 3–105 μm in depth, (d) cell 4–38 μm in depth.

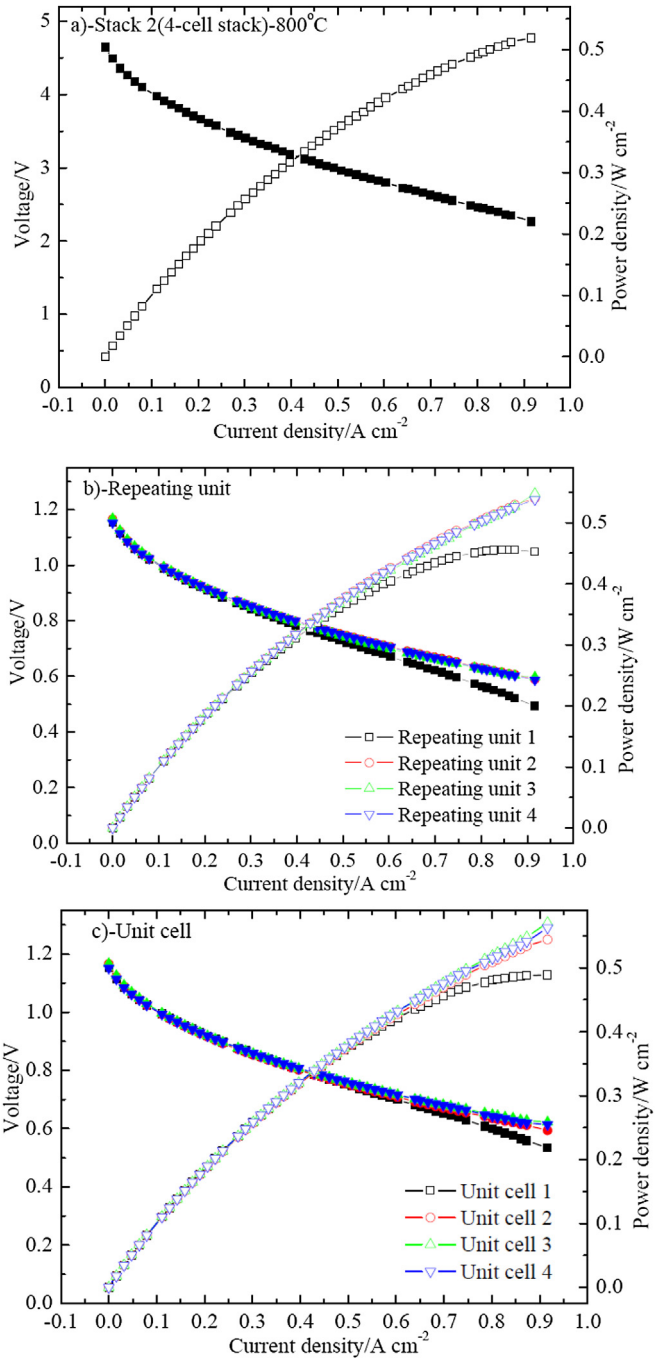


**Fig. 13.** *I–V* curves of stack 2 and its corresponding repeating unit and unit cell: (a) stack 2, (b) repeating unit, (c) unit cell.

### 3.3. Analysis for the influence of contact area and depth on the stack performance

Fig. 18 shows the schematic diagram of the electro motion at the interface contact between the metal interconnect and the CCCL in stack. When the height of the protrusion on the interconnect (the protrusion on the interconnect in the experiment is the metal mesh) embedded into the CCCL from the active cathode is $l$, then the width and number for the protrusion on the interconnect embedded to the CCCL is $a$, $N_1$ and $N_2$. When the thickness of the CCCL of the unit cell is a constant value, a smaller $l$ indicates a larger $h$, which is the contact depth between the interconnect and the

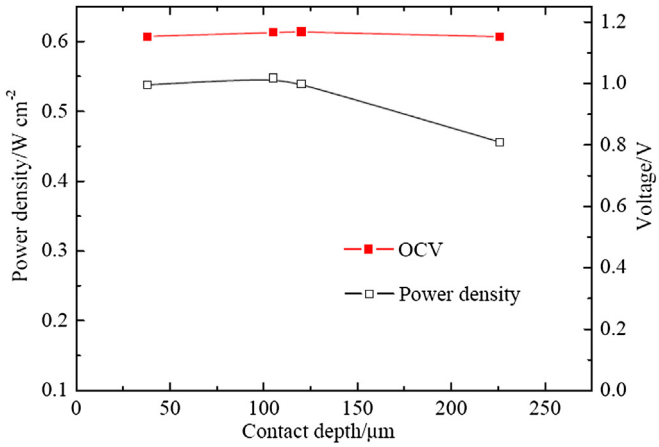


**Fig. 14.** The relationship between the MOPD of repeating unit in stack 2 and the contact depth.

CCCL. A larger $a$, $N_1$ and $N_2$ indicates a larger $S$, which is the contact area between the interconnect and the CCCL. According to the working principle of SOFC [27,28], the electrons produced by the cell anode are transferred to the CCCL via the protrusion on the interconnect (indicated by the arrows in Fig. 18) and reaches the triple-phase boundary of the active cathode to initiate reduction reaction with oxygen. Therefore, the electrons need to undergo a passage process through ohmic resistance before reaching the triple-phase boundary of the active cathode. As Fig. 18 shows, $R_1$ represents the resistance produced in the process in which the electrons are transferred from the anode side of the interconnect to the contact point between the cathode side of the interconnect and the CCCL, whereas $R_2$ represents the resistance produced in the process in which the electrons are transferred from the contact point between the interconnect and the CCCL to the triple-phase boundary of active cathode. Then, the total resistance $R$ can be defined as that the resistance produced in the electron transfer from the anode side of interconnect to the triple-phase boundary of the active cathode of the cell, which is equal to the value for the series connection of $R_1$ and $R_2$; thus, $R = R_1 + R_2$, as seen in Fig. 18. The contact resistance between the interconnect and the CCCL can be seen as the result of the parallel connection of numerous ohmic resistors. Fig. 18 shows that the resistance value of $R_1$ is mainly

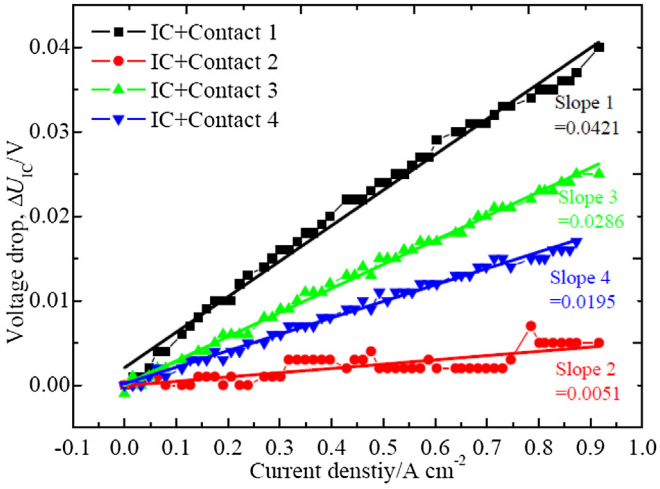


**Fig. 15.** The voltage drop caused by the interconnect and its contact with the cell cathode ($\Delta U_{IC}$) as current density magnitude varies in stack 2.

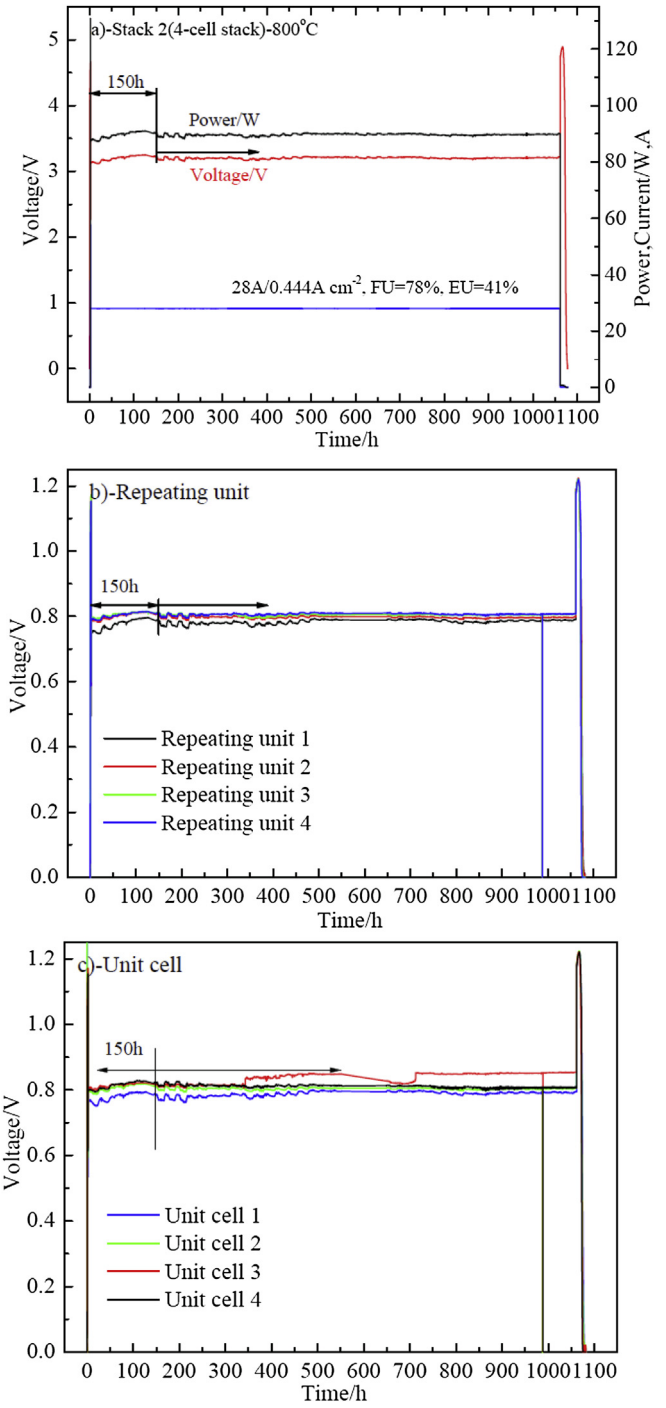


**Fig. 16.** Degradation curve of stack 2 and its corresponding repeating unit and unit cell: (a) stack 2, (b) repeating unit, (c) unit cell.

determined by the resistivity of metal interconnect and metal mesh, whereas that of $R_2$ is mainly determined by the resistivity of LSM.

According to Ohm's Law, $R = \rho l/S$, the magnitude of resistance is co-determined by resistivity ($\rho$), wire length ($l$), and cross-sectional area of the wire ($S$). In this experiment, the cathode and the CCCL are made of the same materials as indicated in the literature [29], and $\rho$ of the materials remains constant above 800 °C. Therefore, when the contact area between the interconnect and the CCCL (but the contact depth is constant) and the depth of interface contact

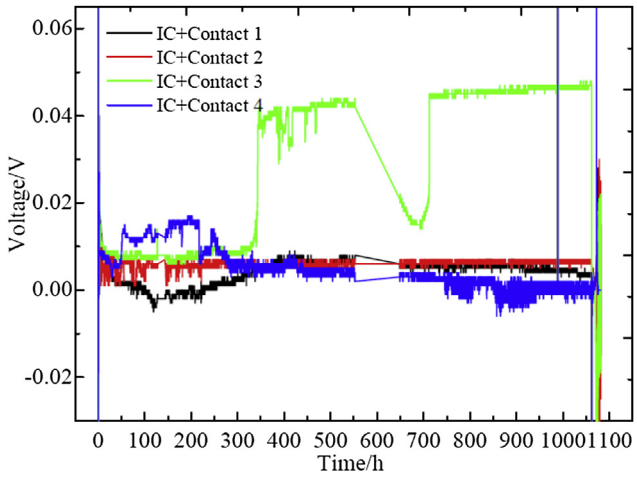


**Fig. 17.** The voltage drop ($\Delta U_{IC}$) jointly contributed by the metal interconnect and its contact with the cell cathode in stack 2.

vary (but the contact area is constant), i.e., when $S$ increases ($l$ remains unchanged) or $l$ decreases ($S$ remains unchanged), $R$ in the stack will both increase. Thus, whether the interface contact area or the depth being increased, an increase in the MOPD of the corresponding cell inside the stack occurs.

However, when the stack operates under constant current, according to the SOFC working principle [27,28] and Joule's Law, $Q = I^2Rt$, the chemical reaction and the current of the cell produce a large amount of heat to increase the temperature on the cathode side of the cell. The smaller the contact area in the stack, the greater the interface resistance and the more heat is produced by the same current magnitude within the same period of time. If the heat produced is not dissipated in a timely manner, a greater increase in temperature is observed on the cathode side of the corresponding unit cell. For the stack with different contact areas, the diagram for pressure application and air distribution in the stack in the testing process (Fig. 4) shows that the cold air enters the stack from bottom to top. Thus, the cold air first reaches repeating unit 1; after heating, it sequentially passes repeating units 2, 3, and 4. According to the literature [30], when the cold air sequentially passes repeating units 1, 2, 3, and 4, the temperature of the corresponding inlet also increases. Thus, when the heat produced by the chemical reaction and the current effect is constant, the heat taken away by the air will decrease in sequence. The surface temperature on the cathode side of repeating units 1, 2, 3, and 4 accordingly increase. The

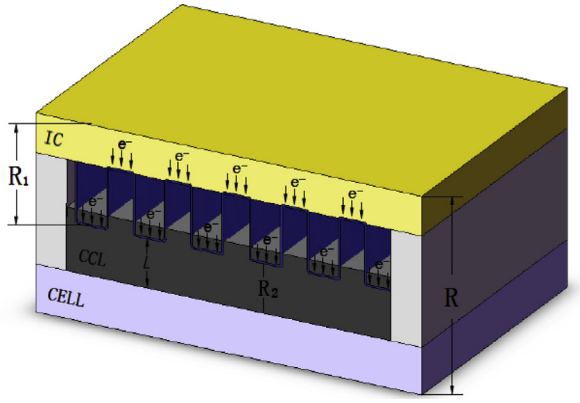


**Fig. 18.** Schematic diagram of the electron motion at the interface between the metal interconnect and the CCCL inside stack.

working temperature of the stack in this paper is 800 °C. Thus, when the surface temperature on the cell cathode side exceeds 800 °C, according to the literature [29], the resistivity of LSM remains unchanged, which means $R_2$ stays the same. Both the interconnect and the metal mesh are made of metal materials, and the resistivity will slowly increase with increasing temperature [31]. This result shows that the gradual increase of $R_1$ can lead to the growth of interface resistance $R$ and the degradation in the repeating unit and its unit cell in the stack.

Therefore, in stack 1 with different contact areas, as the contact area increases, the degradation rate of the repeating unit in stack 1 also increases. When the contact area increases from 38.84% to 45.37%, the repeating unit with a contact area of 45.37% is at the top of the stack and cold hydrogen is fed into the stack from top to bottom. Thus, the contact area has the greatest cooling effect on this repeating unit, which can cause lower temperature compared with that in other repeating units. The increase in amplitude for the interface resistance of this repeating unit is also smaller than that for other repeating units, and the corresponding degradation rate is the smallest. Similarly, when we use the repeating unit with a uniform contact area of 45.37% to assemble stack 2, the ohmic resistance of the repeating unit in stack 2 is lower than that of the repeating unit with a contact area of 45.37% in stack 1. Under the same current magnitude, less heat is generated. At the same time, the generated heat is equal to the amount of heat taken away by the air, resulting in a constant temperature of the electrode inside the repeating unit. The conductivity of the cell cathode LSM and the metal interconnect and its metal mesh does not significantly change. Thus, no degradation is observed in the repeating unit and its unit cell in stack 2.

## 4. Conclusion

A 4-cell stack was assembled at a contact depth of 150 μm and contact area of 28.17%, 33.39%, 38.84% and 45.37%, respectively. Under 800 °C, the MOPD of the stack was 0.428 W $cm^{-2}$. The MOPDs for the repeating unit inside stack increased from 0.315 W $cm^{-2}$ to 0.428 W $cm^{-2}$, 0.496 W $cm^{-2}$, and then decreased slightly to 0.482 W $cm^{-2}$ with the corresponding increasing contact area, showing a convex parabolic relation of the MOPD to the interface contact area. After operating for 972 h under the current density of 0.476 A $cm^{-2}$ and a fuel utilization efficiency of 41.8%, the total degradation rate was 3.1%/1000 h. The degradation rates corresponding to the repeating units also increased from 3.02%/1000 h to 3.25%/1000 h, 3.37%/1000 h, and then decreased to 2.28%/1000 h. Accordingly, the interface contact area of 45% was the optimum value for stack assembling.

The optimum contact area of 45% and the actual interface contact depth of 38, 105, 120, and 226 μm were adopted to assemble a second 4-cell stack, the total MOPD reached 0.519 W $cm^{-2}$ under 800 °C, increasing 21.3% in power density comparing with that of the stack with different contact area. The MOPDs for the stack repeating units increased from 0.538 W $cm^{-2}$ to 0.548 W $cm^{-2}$, and then decreased to 0.540 W $cm^{-2}$ and 0.456 W $cm^{-2}$ with the corresponding increasing contact depth. A convex parabolic relation of the MOPD for repeating unit inside stack to the interface contact depth between interconnect and cell cathode was also found. The stack operated for 1060 h showing without any degradation under 0.8 V unit-cell voltage, 0.444 A $cm^{-2}$ current density, and 78% fuel utilization rate. Therefore, the interface contact area of 45% and the interface contact depth of 105 μm were the optimum parameters for SOFC stack assembling in this investigation.

## Acknowledgment

The authors would like to thank the National High-Tech Research and Development Program of China (863 project No.2011AA050703) and China Postdoctoral Science Foundation (2012M521208).

## References

[1] T.L. Wen, D. Wang, H.Y. Tu, M. Chen, Z. Lu, Z. Zhang, H. Nie, W. Huang, Solid State Ionics 152–153 (2002) 399–404.
[2] J. Myung, H.J. Ko, H.G. Park, M. Hwan, S.H. Hyun, Int. J. Hydrogen Energy 37 (2012) 498–504.
[3] H. Moon, S.D. Kim, E.W. Park, S.H. Hyun, H.S. Kim, Int. J. Hydrogen Energy 33 (2008) 2826–2833.
[4] C. Zhang, Y. Lin, R. Ran, Z. Shao, Int. J. Hydrogen Energy 35 (2010) 8171–8176.
[5] M.L. Liu, Z. Lv, B. Wei, X.Q. Huang, Y.H. Zhang, W.H. Su, Solid State Ionics 181 (2010) 939–942.
[6] H.J. Zhai, W.B. Guan, Z. Li, C. Xu, W.G. Wang, J. Korean Ceram. Soc. 45 (2008) 777–781.
[7] J.W. Wu, X.B. Liu, J. Mater. Sci. Technol. 26 (2010) 293–305.
[8] Y.J. Xu, Z.Y. Wen, S.R. Wang, T.G. Wen, Solid State Ionics 192 (2011) 561–564.
[9] P. Metzger, K.A. Friedrich, H. Müller-Steinhagen, G. Schiller, Solid State Ionics 177 (2006) 2045–2051.
[10] M.E. Lynch, M.L. Liu, J. Power Sources 195 (2010) 5155–5166.
[11] K.Channa R. De Silva, B.J. Kaseman, D.J. Bayless, Int. J. Hydrogen Energy 36 (2011) 779–786.
[12] T. Dey, P.C. Ghosh, D. Singdeo, M. Bose, R.N. Basu, Int. J. Hydrogen Energy 36 (2011) 9967–9976.
[13] N.H. Menzler, F. Tietz, S. Uhlenbruck, H.P. Buchkremer, D. Stove, J. Mater. Sci. 45 (2010) 3109–3135.
[14] L.T. Wilkinson, J.H. Zhu, J. Electrochem. Soc. 156 (2009) B905–B912.
[15] C. Chervin, R.S. Glass, S.M. Kauzlarich, Solid State Ionics 176 (2005) 17–23.
[16] S.P. Jiang, J.G. Love, L. Apateanu, Solid State Ionics 160 (2003) 15–26.
[17] J.I. Gazzarri, O. Kesler, J. Power Sources 176 (2008) 138–154.
[18] W. Konga, J.Y. Li, S.X. Liuc, Z.J. Lin, J. Power Sources 204 (2012) 106–115.
[19] W.B. Guan, H.J. Zhai, L. Jin, T.S. Li, W.G. Wang, Fuel Cells 11 (2011) 445–450.
[20] W.B. Guan, L. Jin, X. Ma, W.G. Wang, Fuel Cells 12 (2012) 1085–1094.
[21] C.R. He, W.G. Wang, J.W.Y. Xue, J. Power Sources 196 (2011) 7639–7644.
[22] C.R. He, W.G. Wang, Fuel Cells 9 (2009) 630–635.
[23] W.B. Guan, H.J. Zhai, L. Jin, C. Xu, W.G. Wang, Fuel Cells 12 (2012) 24–31.
[24] F. Z, M.D. Merrill, J.C. Tokash, T. Saito, S. Cheng, M.A. Hickner, B.E. Logan, J. Power Sources 196 (2011) 1097–1102.
[25] J. Yamanis, J. Hawkes, L.C. JR, C.E. Bird, E.Y. Sun, P.F. Croteau, Fuel Cell Repeater Unit, Pub. No.: US 2010/0248065 A1, Sep. 30, 2010.
[26] K.S. Weil, K.D. Meinhardt, V.L. Sprenkle, Cassettes for Solid-oxide Fuel Cell Stacks and Methods of Making the Same, Patent No.: US 8293426 B2, Inventors Assigne: Battelle Memorial Institute, Richland, WA (US), Oct. 23, 2012.
[27] A.V. Virkar, J. Power Sources 172 (2007) 713–724.
[28] R. Kandepu, L. Imsland, B.A. Foss, C. Stiller, B. Thorud, O. Bolland, Energy 21 (2007) 406–417.
[29] J.X. Wang, Y.K. Tao, J. Shao, W.G. Wang, J. Power Sources 186 (2009) 344–348.
[30] H. Apfel, M. Rzepka, H. Tu, U. Stimming, J. Power Sources 154 (2006) 370–378.
[31] K. Matsugi, Y. Wang, T. Hatayama, O. Yanagisawa, K. Syakagohri, J. Mater. Process. Technol. 135 (2003) 75–82.